Carbohydrate Polymers 92 (2013) 33–39

Contents lists available at SciVerse ScienceDirect

Carbohydrate Polymers

journal homepage: www.elsevier.com/locate/carbpol

Mucoadhesive nanoparticles made of thiolated quaternary chitosan crosslinked with hyaluronan

Ylenia Zambito[a,*], Francesca Felice[b], Angela Fabiano[a], Rossella Di Stefano[b], Giacomo Di Colo[a]

[a] Department of Pharmaceutical Sciences, University of Pisa, Via Bonanno 33, 56126 Pisa, Italy
[b] Cardiothoracic and Vascular Department, University of Pisa, Via Paradisa, 2, 56126 Pisa, Italy

ARTICLE INFO

Article history:
Received 12 July 2012
Received in revised form
12 September 2012
Accepted 13 September 2012
Available online 23 September 2012

Keywords:
Thiolated quaternized chitosan
Chitosan–hyaluronan nanoparticles
Ionotropically cross-linked nanoparticles
Mucoadhesive nanoparticles
Nanoparticle cellular uptake

ABSTRACT

Mucoadhesive polymeric nanoparticles intended for drug transport across the gastrointestinal mucosa were prepared from quaternary ammonium–chitosan conjugates synthesised from reduced-MW chitosan (32 kDa). Conjugates contained pendant moieties of 2–4 adjacent diethyl-dimethylene-ammonium groups substituted on repeating units (26–55%). Conjugates were thiolated via amide bonds with thioglycolic acid to yield products with thiol content in the 35–87 μmol/g range. Nanoparticles with mean size in the 270–370 nm range and positive zeta-potential (+3.7 to +12.5 mV) resulted from ionotropic gelation of the thiolated conjugates with de-polymerised hyaluronic acid (470 kDa). The nanoparticles were fairly stable in size and thiol content and showed a significant mucoadhesivity, matching and even exceeding that of the constituent polymers. Nanoparticles were internalised by endothelial progenitor cells in direct relation to their surface charge intensity. Nanoparticle uptake significantly improved cell viability and resistance to oxidation. The lyophilised nanoparticles were re-dispersible and could make a manageable formulation for oral use.

1. Introduction

Mucoadhesive nanoparticulate systems for drug delivery by the oral route, that is the preferred route for systemic drug administration, have raised widespread interest for their recognised potential for improving the bioavailability of drugs with low mucosal permeability and/or lack of chemical stability in the gastrointestinal (GI) environment (Dünnhaupt et al., 2011; Ponchel, Montisci, Dembri, Durrer, & Duchêne, 1997; Sakuma et al., 2002; Sarmento et al., 2007; Takeuchi, Yamamoto, & Kawashima, 2001). Adhesion to mucus can slow down particle transit across the GI tract, thus prolonging residence of the carried drug at the absorption site and realising steep drug concentration gradients across the mucous membrane for a prolonged time (Dünnhaupt et al., 2011). Nanoparticles can also increase oral drug bioavailability by protecting the entrapped drug from degradation (Dünnhaupt et al., 2011; Ponchel et al., 1997; Sakuma et al., 2002; Sarmento et al., 2007). The prime consideration, when aiming at preparing mucoadhesive polymeric nanoparticles, is the basic material, which is supposed to be a mucoadhesive, biocompatible and biodegradable polymer. Chitosan derivatives positively charged on their repeating units are candidate materials in this respect. Our group have synthesised chitosan derivatives bearing short pendant chains containing a small number of adjacent quaternary ammonium groups, partially substituted on the chitosan repeating units (Zambito, Uccello-Barretta, Zaino, Balzano, & Di Colo, 2006). A comparatively high fraction of free, unsubstituted primary amino groups was left on the chitosan derivative backbone, available for covalent attachment of thiol-bearing compounds, via formation of 3-mercaptopropionamide moieties. This has, in fact, led to water-soluble thiolated quaternary ammonium–chitosan conjugates, the epithelial permeability-enhancing potential of which was tested using the Caco-2 cell monolayer and the excised rat jejunum as substrates (Zambito et al., 2009). On the basis of the obtained results the quaternary ammonium groups of these derivatives were ascribed the ability to reversibly open the epithelial tight junctions and also perturb the plasma membrane of the epithelial cells. On their part the thiol groups were believed to keep the polymer adherent to the epithelium by reacting with the thiols of the epithelial mucus to form disulphide bonds, thus favouring the permeability-enhancing action of the positive ions. This synergistic action points to the above chitosan derivatives as promising basic materials for preparing mucoadhesive bioactive nanoparticles. However, the polymers obtained by Zambito et al. (2009) have resulted, as such, unsuitable for this purpose, indeed, their ionotropic gelation with tripolyphosphate, used in the past to obtain nanoparticles from polycationic chitosan or N-trimethylchitosan (Sandri et al., 2007), yielded particles beyond the nanosize limit (unpublished results), possibly due to an exceedingly high molecular weight of the starting chitosan (590 kDa, viscometric). In fact it has been stated that 500 nm is

* Corresponding author. Tel.: +39 050 2219657; fax: +39 050 2219660.
E-mail address: zambito@farm.unipi.it (Y. Zambito).

0144-8617/$ – see front matter © 2012 Elsevier Ltd. All rights reserved.
http://dx.doi.org/10.1016/j.carbpol.2012.09.029

the upper size limit for nanoparticles being able to pass across the intestinal mucus layer by endocytosis (Jani, Halbert, Langridge, & Florence, 1990).

Hence, the present work was aimed at (1) obtaining quaternary ammonium–chitosan conjugates starting from de-polymerised chitosan; (2) studying the effects of the reaction conditions, especially temperature, on the structures of products and their reproducibility; (3) introducing thiol groups on the above conjugates via formation of amide bonds with thioglycolic acid; (4) using the resulting thiolated derivatives to prepare stable nanoparticles of adequate size by ionotropic gelation with de-polymerised hyaluronic acid, which is a mucoadhesive polyanionic polysaccharide containing glucuronic acid units, and chemical crosslinking by formation of interchain disulphide bridges from thiol oxidation (Chang et al., 2012); (5) characterising nanoparticles for size and size stability, zeta potential, cytotoxicity, aptitude to be internalised by endothelial progenitor cells, mucoadhesivity compared to the component polymers; (6) planning a manageable formulation of nanoparticles for oral application.

2. Materials and methods

2.1. Materials

The following materials were used. Thioglycolic acid (TGA), 1-ethyl-3-(3-dimethylaminopropyl) carbodiimide hydrochloride (EDAC), fluorescein isothiocyanate (FITC), cellulose membrane tubing MW cut-off 12.5 kDa; (all from Sigma); 2-diethylaminoethyl chloride (DEAE-Cl) hydrochloride (Fluka); hyaluronic acid (HA), MW 950 kDa (Contipro, Dolní Dobrouč, Czech Republic); chitosan minimum 90% deacetylated from shrimp shell (Chitoclear FG90, Primex, Drammen, Norway). The commercial chitosan had an average viscometric molecular weight of 590 kDa and a deacetylation degree, determined by IR or NMR, of 90% or 82% (Zambito et al., 2006). Its MW was reduced by oxidative depolimerisation (see, e.g., Janes & Alonso, 2003; Mao et al., 2004), to obtain rCh (viscometric MW, 32 kDa). The MW of HA was reduced by acid degradation, according to Shu, Liu, Luo, Roberts, and Prestwich (2002), to obtain rHA (viscometric MW, 470 kDa). The viscometric MWs of rCh and rHA were determined by an Ostwald U-tube capillary viscometer (Cannon-Fenske series ASTM 75), following the procedure reported by Khalid, Ho, Agnely, Grossiord, and Couarraze (1999), for rCh in 0.1 M acetic acid/0.2 M NaCl, and that reported by Tadmor, Chen, and Israelachvili (2002), for rHA in 0.1 M NaCl. Quaternary ammonium-rCh conjugates (QA-rCh) were synthesised by reacting DEAE-Cl with rCh, through a procedure similar to that described by Zambito et al. (2006) and Zambito, Zaino, Uccello-Barretta, Balzano, and Di Colo (2008), keeping the pH at 8 and controlling the temperature at 50 °C (product code, QA-rCh50) or 60 °C (product code, QA-rCh60). Before use, the cellulose membrane was soaked at least 24 h in water. All aqueous solutions/dispersions were prepared with freshly distilled water.

2.2. Covalent attachment of thiol groups on QA-rCh conjugates

Thiolation of QA-rCh derivatives was achieved by the attachment of TGA to unsubstituted primary amino groups still present on the QA-rCh chains, via formation of amide bonds mediated by EDAC (Kast & Bernkop-Schnürch, 2001).

EDAC was added to 25 mL of a clear 2% (w/w) QA-rCh50, or QA-rCh60, aqueous solution, up to a concentration of 50 mM. After complete dissolution of EDAC an excess of TGA (0.8 g) was added and the pH adjusted to 5 with 1 M NaOH. The reaction mixture was incubated 3 h at ambient temperature under stirring, then it was dialysed for 3 days. The external phase of dialysis was changed daily: the first day it was 5 mM HCl; the second day, 5 mM HCl containing 1% NaCl; the third day, 5 mM HCl. After dialysis the polymer solution in the tubing was lyophilised to obtain the purified thiolated derivatives, QA-rCh50-SH and QA-rCh60-SH, which were stored at −20 °C in the dark. The procedure for thiolation of QA-rCh50 and QA-rCh60 was repeated as described above, except that EDAC was not added to the mixture.

2.3. Determination of thiol and disulphide content of QA-rCh-SH derivatives

To determine the thiol groups the polymer (15 mg) was dissolved in 10 mL of water, 1% starch aqueous solution (1 mL) was added, the pH was adjusted to 3 with 1 M HCl, and the solution was titrated with 1 mM aqueous iodine until a permanent light blue discolouration was observed (Kast & Bernkop-Schnürch, 2001). The determination of the thiol content was repeated after about a year of storage at −20 °C in the dark. To determine the disulphide groups, these were reduced to thiols by adding 8 mL of 10% aqueous sodium borohydride to a solution of 15 mg polymer in 2 mL of water, and stirring for 1 h. Then the excess sodium borohydride was destroyed by making the solution to pH 3 with 1 M HCl and the thiol content was determined by iodometric titration as described above. The disulphide content was derived from the difference between the thiol contents of reduced and not reduced QA-rCh-SH derivatives. The free thiol and disulphide contents were expressed either as degree of substitution (%) on a polymer repeating unit basis or μmol per g of polymer. The products obtained without using the catalyst EDAC, when titrated with iodine showed an insignificant thiol content, thus proving the validity of the procedure for purification of polymers from TGA, described in Section 2.2.

2.4. FITC-labelling of polymers

A previously described procedure was followed (Clausen & Bernkop-Schnürch, 2000; Clausen & Bernkop-Schnürch, 2001; Di Colo, Zambito, Zaino, & Sansò, 2009).

2.5. Preparation and characterisation of nanoparticles based on QA-rCh-SH derivatives

Aliquots (50 μL) of 0.025 mg/mL rHA solution in isotonic phosphate buffer pH 7.4, 0.13 M (PB) were consecutively added to 10 mL of 2 mg/mL of each FITC-labelled or unlabelled QA-rCh-SH derivative in PB under continuous stirring, analysing the system for dispersed particles by light scattering (Nano Z690 Malvern) after each addition. The addition was stopped when the formation of nanoparticles in the 270–370 nm size range was observed. The zeta potential of particles was also measured. The total volume of rHA solution was 0.7 mL, with either FITC-labelled or unlabelled QA-rCh60-SH, used for the preparation of nanoparticles of NP1 type, or 1.1 mL with either FITC-labelled or unlabelled QA-rCh50-SH, used to obtain nanoparticles of NP2 type. The nanoparticle dispersions were analysed, hourly for 6 h and after 24 h from preparation, for mean particle size. The thiol content of nanoparticle dispersions prepared by the above procedure was determined by iodometric titration, as described in Section 2.3, and expressed either as μmol per g of rCh derivative used to prepare the nanoparticles, or degree of substitution (%) on a rCh-derivative repeating unit basis. Interference from the rHA immobilised within nanoparticles could be ruled out by checking the reaction with iodine of a corresponding concentration of rHA in solution. The thiol content of nanoparticles was compared with that of corresponding amounts of the respective constituent polymers. The thiol content was checked after 24 h from preparation of nanoparticles. To obtain stable and manageable formulations the nanoparticle dispersions

were lyophilised (Virtis, Advantage-53, Steroglass, Perugia, Italy. Freezing step: −35 °C in 180 min; drying cycle steps: (1) −30 °C, 360 min; (2) −10 °C, 360 min; (3) 10 °C, 240 min; (4) 25 °C, 180 min). The dispersions were regenerated from the respective lyophilised products by adding water, and gently mixing, immediately after lyophilisation or after about one month of storage either in a desiccator at ambient temperature or in a freezer at −20 °C. The regenerated dispersions were checked for particle size.

2.6. Ex vivo mucoadhesivity studies

The mucoadhesivity of nanoparticles was compared with that of the constituent QA-rCh-SH and rHA, and that of non-thiolated QA-rCh polymers (all FITC-labelled and dispersed/dissolved in PB) by the following ex vivo procedure, modified from Pimienta, Chouinard, Labib, and Lenaerts (1992).

The intestinal mucosa was excised from non fasting male Wistar rats weighing 250–300 g. They were treated as prescribed in the publication 'Guide for the care and use of laboratory animals' (NIH Publication No. 92-93, revised 1985). All experiments were carried out under veterinary supervision, and the protocols were approved by the ethical scientific committee of the University of Pisa. After sacrificing the rats, the first 50 cm of small intestine was immediately removed. Four 10-cm segments were cut out of the excised intestine, opened by longitudinal cutting, and the mucosa gently rinsed free of luminal contents with PB. Each segment was then immersed in 1 mL of the polymer solution, or nanoparticle dispersion, to be tested, so as to allow sample penetration into the intestinal lumen to come into contact with the mucosa. Incubation at 37 °C, under bubbling of a mixture of 95% O_2 and 5% CO_2, lasted 3 h with no damage to the mucosa (Zambito et al., 2009). Then, 20 μL were withdrawn, appropriately diluted with PB, and the concentration of the relevant FITC-labelled material was measured fluorimetrically with reference to the relative calibration curve. Each sample to be tested for mucoadhesivity was also incubated, in the above-described conditions, with a 10-cm intestinal segment closed at both ends by tying with cotton thread, in order to allow sample contact with only the muscle side of the intestinal segment, while preventing sample penetration into the intestinal lumen. The adsorbed mass fraction was calculated as the percent difference between the concentrations of FITC-labelled material before and after incubation.

2.7. Isolation and culture of endothelial progenitor cells (EPCs)

EPCs were isolated from total peripheral blood mononuclear cells (PBMCs) after 3 days of culture in a selective medium, as previously described (Di Stefano et al., 2002). Briefly, PBMCs of a healthy human donor were isolated by density gradient centrifugation on Lymphoprep (Nycomed, Oslo, Norway; density 1.077 g/ml) at 400 × *g* for 30 min at room temperature, according to the manufacturer's protocol. After centrifugation, the interface cells were carefully removed and transferred to a new conical tube. Cells were washed twice with PBS, centrifuged at 300 × *g* for 10 min, and then suspended in a mixture of 9 mL water and 3 mL KCl 0.6 M, made to a final volume of 50 mL with PBS. Isolated PBMCs (10^6 cells/cm^2) were plated on 96-well plates (Greiner Bio One, Frickenhausen, Germany) coated with fibronectin and maintained in endothelial basal medium (EBM-2, Cambrex, Walkersville, MD) supplemented with EGM-2-MV-Single Quots containing human endothelial growth factor, hydrocortisone, insulin-like growth factor, fibroblast growth factor, vascular endothelial grow factor (VEGF), antibiotics, and 5% fetal bovine serum (FBS, Cambrex). Cells were cultured at 37 °C with 5% CO_2 in a humidified atmosphere.

2.8. EPC treatment

After 4 days of culture, non-adherent cells were removed by washing with PBS and adherent cells were incubated for 3 or 12 h with a nanoparticle dispersion of the NP1, or NP2 type, prepared as described in Section 2.5. and diluted 25 times with a serum-free medium. At the end of the treatment, cells were washed twice with PBS and either immediately analysed for viability, or subjected to 1-h incubation with 1 mM H_2O_2 before viability testing.

2.9. EPC viability tests

Cell viability was tested by the WST-1 assay. Viability was expressed as percent of viable cells, calculated from the ratio of formazan dye absorbance after cell treatment with nanoparticles, to mean absorbance for the untreated control.

2.10. Intracellular uptake of nanoparticles

EPCs were incubated for 3 or 12 h in a serum-free medium with either fluorescent NP1 or NP2. Intracellular uptake was observed under a fluorescence microscope (Carl Zeiss, Germany) at 10× magnification, after nuclear labelling of EPCs with Hoechst 33258 (1:1000) (Sigma–Aldrich).

2.11. Statistical analysis

All results are presented as mean ± SD of *n* independent experiments. The results of the cell viability tests were compared using analysis of variance (ANOVA) for repeated measurements. Post hoc analysis was performed by Bonferroni's multiple comparison test.

3. Results and discussion

3.1. Synthesis of QA-rCh conjugates

The products obtained by reacting the reduced-MW chitosan (rCh) with DEAE-Cl had the basic structure of quaternary ammonium–chitosan conjugates, precisely, *N*,*O*-[*N*,*N*-diethylaminomethyl(diethyldimethylene ammonium)$_n$]methyl chitosan, coded QA-rCh. They were similar in structure to the derivatives that were obtained by Zambito et al. (2006, 2008) starting from commercial chitosan, having a much higher MW, as shown by the NMR spectra being similar (not reported). The conjugates would bear moieties made of a small number of adjacent quaternary ammonium groups, partially substituted on the rCh repeating units. The degree of substitution (DS) and the mean number of quaternary ammonium groups in each substituted moiety (*n*) strongly depended on the pH of the reaction mixture, which required being strictly controlled at 7 or 8 for the reaction being reproducible (Zambito et al., 2008). In the present work the reaction was carried out starting from rCh in view of obtaining conjugates of comparatively small MW, whereby to prepare nanoparticles of appropriate size. The effect of lowering the reaction temperature below 65 °C, that is the value used by Zambito et al. (2008), was investigated, while the pH of the reaction mixture was controlled at 8 for the sake of reproducibility. The reaction, when conducted at 50 or 60 °C, reproducibly yielded conjugates of the QA-rCh type, whereas at 40 °C the reaction either did not occur or was not reproducible. The respective DS and *n* values for the two derivatives, determined by NMR and found in Table 1, are significantly different, the higher DS corresponding to the lower *n*. Also listed in the table are the DS and *n* values for N^+-Ch-8, that is the quaternary ammonium–chitosan conjugate obtained by Zambito et al. (2008) from the commercial chitosan at pH 8 and 65 °C. Such values, although statistically hardly distinguishable from the

Table 1
Effect of reaction temperature (T) on degree of acetylation (DA), degree of substitution (DS), number of quaternary ammonium groups in substituted moieties (n), of quaternary ammonium–chitosan conjugates. Means ± SD of 3 batches.

T (°C)	Polymer code	DA (%)	DS (%)	n
40	nr[a]	nr[a]	nr[a]	nr[a]
50	QA-rCh50	12.3 ± 3.6	26.4 ± 7.0	3.8 ± 0.3
60	QA-rCh60	10.5 ± 0.8	55.3 ± 3.2	2.1 ± 0.1
65[b]	N^+-Ch-8[b]	18[b]	59.2 ± 4.5[b]	1.7 ± 0.1[b]

[a] Not reported as the reaction was not reproducible.
[b] Data from Zambito et al. (2008).

respective values for QA-rCh60, are in agreement with the trend of DS to increase and of n to decrease with increasing temperature. This observation suggests that the growth of pendant quaternary ammonium moieties required a lower energy of activation than quaternary ammonium substitution on glucosamine units, irrespective of the length of the chitosan chain. Interestingly, it can be calculated that whichever quaternary ammonium–chitosan conjugate listed in Table 1, synthesised in different temperature conditions, carried an average of one positive charge per repeating unit, which is possibly the maximum affordable for this type of polymers.

3.2. Covalent attachment of thiol groups on QA-rCh derivatives

It appears from the DS and acetylation values listed in Table 1 for the QA-rCh derivatives that significant fractions of unsubstituted glucosamine units, namely, about 60%, with QA-rCh50, and about 35%, with QA-rCh60, were still present in the polymer chains. These units were potentially available for covalent attachment of thiol groups via formation of amide bonds between the primary amino group of glucosamine and the carboxyl group of TGA. Our analysis in fact has shown the presence of covalently bound thiol and disulphide groups, the fractions of which in the thiolated products are found in Table 2. Sodium chloride was introduced in the receiving phase of the dialysis, used to purify the thiolated polymers, in order to facilitate removal of non-reacted anionic TGA and its replacement with chloride ion. An acidic pH was maintained in the course of dialysis because thiol oxidation to disulphide is favoured by neutral/alkaline environments. Nevertheless most thiols actually underwent oxidation, as appears from a comparison between disulphide and thiol content for each thiolated derivative. Despite this, both polymers remained readily water-soluble. The mean thiol and disulphide values for QA-rCh50-SH appear in Table 2 to be about the double of the respective values for QA-rCh60-SH, practically reflecting the ratio between the glucosamine units available for thiolation, present in the respective parent QA-rCh polymers. The thiol content of either thiolated polymer remained virtually unchanged after a year of storage in the lyophilised state at −20 °C in the dark.

3.3. FITC-labelling of polymers

The labelling reaction went to completion, in fact no non-reacted FITC was ever detected. The fluorophore bound to the polymer was calculated at about 5% of the total mass (about 0.13 mmol/g).

3.4. Characteristics of nanoparticles from QA-rCh-SH derivatives (NP1, NP2)

Nanoparticles resulted from the interaction between each polycationic derivative and the polyanion rHA. The physical characteristics of nanoparticles, measured immediately after their preparation, are listed in Table 3. The mean size of nanoparticles determined immediately after their preparation, 24 h thereafter, and after re-dispersion immediately after lyophilisation, or after one month of storage of the lyophilisate in a freezer at −20 °C was always within the 270–370 nm range. The polydispersity index, seen in Table 3 for both nanoparticle types, shows acceptable values for discrete particles. On the other hand, when the lyophilisate was stored in a desiccator at ambient temperature for one month, the mean size of the regenerated nanoparticles was beyond the above range (466 nm). The zeta potential of the nanoparticles was positive, as shown in Table 3. The DS and n values listed in Table 1 suggest an average of one positive charge per repeating unit for the different quaternary ammonium–chitosan conjugates, and likewise, for their thiolated derivatives. Hence the zeta potential values listed in Table 3 indicate that the electrostatic interaction with the anionic crosslinker, rHA, was stronger where the net positive charge was lower, i.e., in the case of NP2.

The thiol contents of nanoparticles, seen in Table 2, appear not to significantly differ from those of the respective constituent polymers, apparently because no further thiol oxidation, and hence, stabilisation by disulphide crosslinks, accompanied the formation of nanoparticles. These, nevertheless, were stable enough, as shown by the stability of their mean size for 24 h. The number of free thiols of nanoparticles is seen in Table 2 non to vary significantly over time, at least up to 24 h from preparation, showing promise of contributing to nanoparticle mucoadhesivity.

Table 2
Results of iodometric analysis of thiolated polymers and nanoparticles. Means ± SD of 6 batches.

Product analyzed	Thiol DS[a] (%)	Thiol content (μmol/g)	Disulphide DS[a] (%)	Disulphide content (μmol/g)
QA-rCh60-SH	1.4 ± 0.3	35.0 ± 6.5	8.3 ± 1.6	205.2 ± 39.6
QA-rCh50-SH	2.8 ± 0.4	87.5 ± 14.0	15.8 ± 2.8	490.8 ± 87.7
NP1 immediately after preparation	1.8 ± 0.3	45.2 ± 7.4	nd[b]	nd[b]
NP1 24 h after preparation	1.9 ± 0.3	47.3 ± 7.6	nd[b]	nd[b]
NP2 immediately after preparation	2.8 ± 0.6	85.8 ± 18.9	nd[b]	nd[b]
NP2 24 h after preparation	2.6 ± 0.5	79.9 ± 14.3	nd[b]	nd[b]

[a] Degree of substitution, on a polymer repeating unit basis.
[b] Not determined.

Table 3
Physical characteristics of nanoparticles. Means ± SD of at least 6 replicates of each nanoparticle preparation.

Nanoparticle type	Mean size (nm)	Polydispersity index	Zeta potential (mV)
NP1	287 ± 32	0.465 ± 0.026	+12.5 ± 0.9
NP2	263 ± 21	0.418 ± 0.039	+3.7 ± 0.3

Table 4
Mass fractions of different FITC-labelled polymers adsorbed on rat intestinal mucosa from solutions of different concentrations (C_0). Means ± SD ($n = 3$).

C_0 (mg/mL)	Adsorbed mass fraction (%)				
	QA-rCh50	QA-rCh50-SH	QA-rCh60	QA-rCh60-SH	rHA
0.1	30.0 ± 2.6	41.0 ± 2.0	30.8 ± 1.4	38.0 ± 1.5	14.2 ± 2.4
2.0	48.5 ± 5.3	64.4 ± 2.7	52.7 ± 3.9	69.6 ± 2.0	50.0 ± 0.9

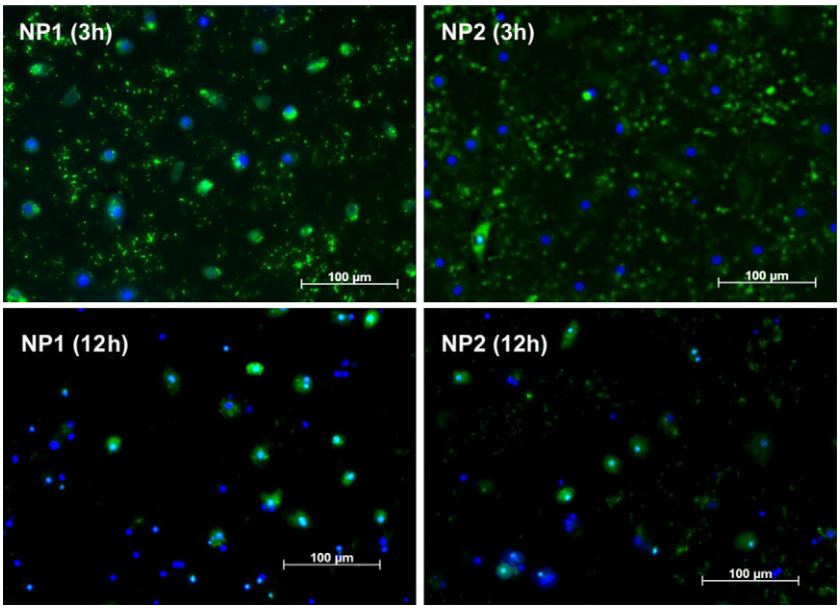

Fig. 1. Images from a fluorescence microscope, showing uptake of FITC-labelled NP1 or NP2 nanoparticle type by endothelial progenitor cells after 3 or 12 h of incubation.

3.5. Mucoadhesion studies

No significant adsorption of the products investigated for mucoadhesivity occurred on the muscle side of the intestinal segment. Conversely, significant mass fractions of nanoparticles and dissolved polymers were adsorbed on the intestinal mucosa from their 0.1 or 2.0 mg/mL dispersions/solutions, as appears from data listed in Tables 4 and 5. The differences between the data about to be discussed are statistically significant (Student's t-test, $P < 0.05$) except in some specified cases. The adsorption of polymers, shown in Table 4, in all cases was significantly stronger with the higher concentration of contact solution. This may be taken as an indication of a co-operative nature of the interaction between the adsorbed macromolecules and the mucus glycoproteins. This was not the case with the nanoparticles, in fact, the adsorption of whichever type on the intestinal mucosa appears from data in Table 5 not to significantly depend on concentration. A comparison of data in Table 4 for the thiolated with the corresponding non-thiolated QA-rCh derivatives shows a significantly stronger mucoadhesivity of the former at either concentration. The synergistic action of quaternary ammonium and thiol moieties to promote the mucoadhesivity of chitosan derivatives has already been pointed out in Section 1. On the other hand, the differences in the DS and n parameters, listed in Table 1, and thiol content, found in Table 2, were reflected in no significant differences in polymer adsorption on intestinal mucosa. The present data supports the assumption that nanoparticles formed from mucoadhesive polymers are themselves mucoadhesive, provided their surface retains the polymer characteristics responsible for mucoadhesion. This is indeed the present case, as demonstrated by the thiol content of nanoparticles, shown in Table 2, and their positive surface charge shown by their zeta potential values reported in Table 3. In fact, a comparison of relevant data in Tables 4 and 5 shows that, at the higher concentration, the adsorbed fractions of nanoparticles are

Table 5
Mass fractions of different FITC-labelled nanoparticles adsorbed on rat intestinal mucosa from dispersions of different concentrations (C_0). Means ± SD ($n = 3$).

C_0 (mg/mL)	Adsorbed mass fraction (%)	
	NP1	NP2
0.1	64.7 ± 4.2	60.3 ± 0.6
2.0	62.0 ± 3.9	59.0 ± 1.3

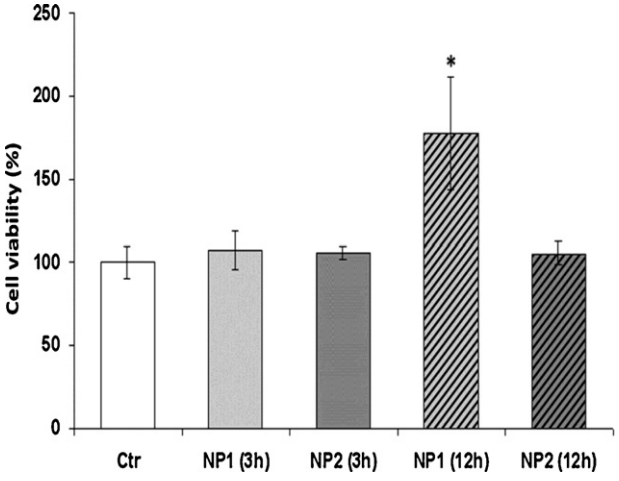

Fig. 2. EPC viability after treatment with NP1 or NP2 nanoparticle type for 3 or 12 h. Viability measured by WST-1 assay and expressed as percent viable cells (ratio of viable number after treatment to that for untreated control). *$P < 0.001$ vs. control ($n = 6$).

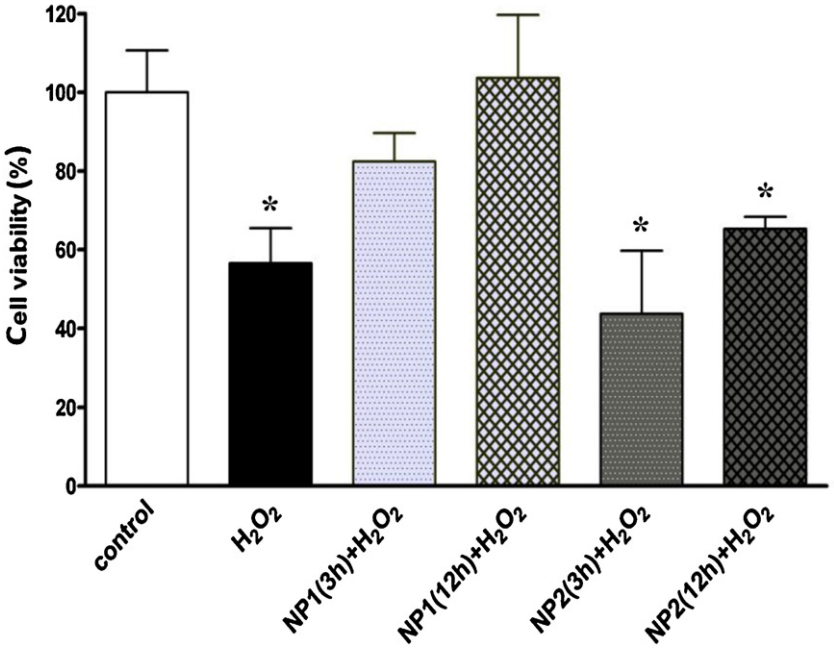

Fig. 3. Nanoparticle effects on oxidative stress. EPCs pre-treated with NP1 or NP2 nanoparticle type for 3 or 12 h and then incubated with 1 mM H_2O_2 for 1 h. Viability measured by WST-1 assay and expressed as percent viable cells (ratio of viable number after treatment to that for untreated control). *$P < 0.001$ vs. control ($n = 6$).

similar to those of the respective constituent polymers, whereas at the lower concentration the nanoparticles are still more mucoadhesive than the constituent polymers.

3.6. Intracellular uptake of nanoparticles

The uptake of nanoparticles by EPCs upon incubation with FITC-labelled NP1 or NP2 for different terms (3 or 12 h) is shown by the images in Fig. 1. After 3 h both nanoparticle types were partially internalised by cells, NP1 being seemingly taken up to a higher extent than NP2. This difference can safely be correlated with the stronger positive surface charge of the former, resulting from the zeta potential measurements reported in Table 3. The images relative to 12 h of incubation show a progress of the internalisation process that still appears more advanced with the NP1 than the NP2 nanoparticle type.

3.7. In vitro cytotoxicity studies

Cytotoxicity of nanoparticles to EPCs was determined by WST-1 colorimetric assay. As shown in Fig. 2, incubation of EPCs with either nanoparticle type for 3 or 12 h did not compromise cell viability. In fact, the results indicate that the EPC viability was significantly ameliorated, compared to the untreated control, by incubation with NP1 for 12 h ($P < 0.001$). These results may be interpreted as a confirmation of a more effective internalisation of NP1 compared with NP2 by EPCs, and of cell viability taking advantage of such an internalisation. This effect may be related to the antioxidant activity of the thiols immobilised on the nanoparticles.

3.8. Nanoparticle effects on oxidative stress

If internalised by EPCs, nanoparticles might protect cells from oxidative stresses by virtue of the antioxidant action of their thiols. In order to verify this hypothesis, the influence of EPC pre-treatment with nanoparticles on the effect of cell incubation with H_2O_2 was investigated. EPCs were pre-treated with either nanoparticle type for 3 or 12 h, and then incubated with 1 mM H_2O_2 for 1 h. As shown in Fig. 3, the treatment with H_2O_2 actually reduced the EPC viability compared to untreated control cells ($P < 0.001$). From the figure also appears that the pre-treatment of EPCs with either nanoparticle type resulted in a higher resistance to the oxidative stress when the time of pre-treatment was longer, although only the pre-treatment with NP1 prevented H_2O_2 from causing any significant cell viability decrease with respect to the untreated control. Considering that NP1 are the nanoparticle type with more aptitude to be internalised, as seen in Fig. 1, the above findings can be taken as a support of the initial hypothesis of this section. The protective effect could be amplified if some antioxidant substance were possibly loaded into nanoparticles.

4. Conclusions

The derivatives obtained by reacting de-polymerised chitosan with DEAE-Cl had the same *N*,*O*-[*N*,*N*-diethylaminomethyl (diethyldimethylene ammonium)$_n$]methyl chitosan structure as those obtained starting from commercial chitosan, although the former had a much lower MW. The reaction temperature exerted a significant influence on such structural properties of the derivatives as the degree of substitution of the positively charged moieties on the chitosan repeating units and the number of adjacent quaternary ammonium groups in each moiety. Yet, the average number of positive charges per repeating unit of polymer was similar, precisely, it was very close to one for whichever derivative. The attempt to immobilise thiol groups on the repeating units of the quaternary ammonium–chitosan conjugates was successful. Nanoparticles of a size adequate for internalisation into cells were obtained by ionotropic gelation of the thiolated derivatives with de-polymerised HA. The nanoparticles were fairly stable as concerns size and thiol content, in fact, chemical crosslinking by formation of interchain disulphide bridges from air-oxidation of thiols did not occur. The nanoparticles showed a significant mucoadhesivity, matching and even exceeding that of the constituent thiolated quaternary ammonium–chitosan conjugates, because the former retained the characteristics, namely, positive surface charge and immobilised thiol groups, that were responsible for the

mucoadhesivity of the latter. The nanoparticles showed an aptitude to be internalised by endothelial progenitor cells, directly related to the intensity of their surface charge. In virtue of the antioxidant function of their thiols, the nanoparticles more apt to be internalised significantly improved cell viability and resistance to oxidation by hydrogen peroxide. It is believed that this beneficial effect could even be strengthened if some biocompatible antioxidant material were possibly loaded into nanoparticles to be carried across the intestinal mucosa into the systemic circulation. The lyophilised nanoparticle dispersion in isotonic phosphate buffer pH 7.4 could be a manageable formulation for oral application, seeing that it might be filled into gastro-resistant capsules and could regenerate the nanosystem in buffered conditions upon contact with the physiologic fluids of the GI tract.

Acknowledgement

The work was funded by the University of Pisa.

References

Chang, D., Lei, J., Cui, H., Lu, N., Sun, Y., Zhang, X., et al. (2012). Disulfide cross-linked nanospheres from sodium alginate derivative for inflammatory bowel disease: Preparation, characterization, and in vitro drug release behavior. *Carbohydrate Polymers*, *88*, 663–669.

Clausen, A. E., & Bernkop-Schnürch, A. (2000). In vitro evaluation of the permeation-enhancing effect of thiolated polycarbophil. *Journal of Pharmaceutical Sciences*, *89*, 1253–1261.

Clausen, A. E., & Bernkop-Schnürch, A. (2001). Thiolated carboxymethylcellulose: In vitro evaluation of its permeation-enhancing effect on peptide drugs. *European Journal of Pharmaceutics and Biopharmaceutics*, *51*, 25–32.

Di Colo, G., Zambito, Y., Zaino, C., & Sansò, M. (2009). Selected polysaccharides at comparison for their mucoadhesiveness and effect on precorneal residence of different drugs in the rabbit model. *Drug Development and Industrial Pharmacy*, *35*, 941–949.

Di Stefano, R., Santoni, T., Barsotti, M. C., Armani, C., Chifenti, B., Guida, C., et al. (2002). Different growth conditions for peripheral blood endothelial progenitors. *Cardiovascular Radiation Medicine*, *3*, 172–175.

Dünnhaupt, S., Barthelmes, J., Hombach, J., Sakloetsakun, D., Arkhipova, V., & Bernkop-Schnürch, A. (2011). Distribution of thiolated mucoadhesive nanoparticles on intestinal mucosa. *International Journal of Pharmaceutics*, *408*, 191–199.

Janes, K. A., & Alonso, M. J. (2003). Depolymerized chitosan nanoparticles for protein delivery: Preparation and characterization. *Journal of Applied Polymer Science*, *88*, 2769–2776.

Jani, P., Halbert, G. W., Langridge, J., & Florence, A. T. (1990). Nanoparticle uptake by the rat gastrointestinal mucosa: Quantitation and particle size dependency. *Journal of Pharmacy and Pharmacology*, *42*, 821–826.

Kast, C. E., & Bernkop-Schnürch, A. (2001). Thiolated polymers—thiomers: Development and in vitro evaluation of chitosan–thioglycolic acid conjugates. *Biomaterials*, *22*, 2345–2352.

Khalid, M. N., Ho, L., Agnely, F., Grossiord, J. L., & Couarraze, G. (1999). Swelling properties and mechanical characterization of a semi-interpenetrating chitosan/polyethylene oxide network. Comparison with a chitosan reference gel. *STP Pharma Sciences*, *9*, 359–364.

Mao, S., Shuai, X., Unger, F., Simon, M., Bi, D., & Kissel, T. (2004). The depolymerization of chitosan: Effects on physicochemical and biological properties. *International Journal of Pharmaceutics*, *281*, 45–54.

Pimienta, C., Chouinard, F., Labib, A., & Lenaerts, V. (1992). Effect of various poloxamer coatings on in vitro adhesion of isohexylcyanoacrylate nanospheres to rat ileal segment under liquid flow. *International Journal of Pharmaceutics*, *80*, 1–8.

Ponchel, G., Montisci, M.-J., Dembri, A., Durrer, C., & Duchêne, D. (1997). Mucoadhesion of colloidal particulate systems in the gastro-intestinal tract. *European Journal of Pharmaceutics and Biopharmaceutics*, *44*, 25–31.

Sakuma, S., Sudo, R., Suzuki, N., Kikuchi, H., Akashi, M., Ishida, Y., et al. (2002). Behavior of mucoadhesive nanoparticles having hydrophilic polymeric chains in the intestine. *Journal of Controlled Release*, *81*, 281–290.

Sandri, G., Bonferoni, M. C., Rossi, S., Ferrari, F., Gibin, S., Zambito, Y., et al. (2007). Nanoparticles based on N-trimethylchitosan: Evaluation of absorption properties using in vitro (Caco-2 cells) and ex vivo (excised rat jejunum) models. *European Journal of Pharmaceutics and Biopharmaceutics*, *65*, 68–77.

Sarmento, B., Ribeiro, A., Veiga, F., Sampaio, P., Neufeld, R., & Ferreira, D. (2007). Alginate/chitosan nanoparticles are effective for oral insulin delivery. *Pharmaceutical Research*, *24*, 2198–2206.

Shu, X. Z., Liu, Y., Luo, Y., Roberts, M. C., & Prestwich, G. D. (2002). Disulfide cross-linked hyaluronan hydrogels. *Biomacromolecules*, *3*, 1304–1311.

Tadmor, R., Chen, N., & Israelachvili, J. N. (2002). Thin film rheology and lubricity of hyaluronic acid solutions at a normal physiological concentration. *Journal of Biomedical Materials Research*, *61*, 514–523.

Takeuchi, H., Yamamoto, H., & Kawashima, Y. (2001). Mucoadhesive nanoparticulate systems for peptide drug delivery. *Advanced Drug Delivery Reviews*, *47*, 39–54.

Zambito, Y., Uccello-Barretta, G., Zaino, C., Balzano, F., & Di Colo, G. (2006). Novel transmucosal absorption enhancers obtained by aminoalkylation of chitosan. *European Journal of Pharmaceutical Sciences*, *29*, 460–469.

Zambito, Y., Zaino, C., Uccello-Barretta, G., Balzano, F., & Di Colo, G. (2008). Improved synthesis of quaternary ammonium–chitosan conjugates (N+–Ch) for enhanced intestinal drug permeation. *European Journal of Pharmaceutical Sciences*, *33*, 343–350.

Zambito, Y., Fogli, S., Zaino, C., Stefanelli, F., Breschi, M. C., & Di Colo, G. (2009). Synthesis, characterization and evaluation of thiolated quaternary ammonium–chitosan conjugates for enhanced intestinal drug permeation. *European Journal of Pharmaceutical Sciences*, *38*, 112–120.